A Modular Micromachined High-Density Connector System for Biomedical Applications

Tayfun Akin, Babak Ziaie,* *Associate Member, IEEE*, Stefan A. Nikles, and Khalil Najafi, *Senior Member, IEEE*

Abstract— **This paper presents a high-density, modular, low-profile, small, and removable connector system developed using micromachining technologies for biomedical applications. This system consists of a silicon or polyimide electrode with one end in contact with the biological tissue and its back-end supported in a titanium base (12.5 mm in diameter and 2.5 mm in height) that is fixed on the test subject. An external glass substrate ($6 \times 6 \times 0.75$ mm^3), which supports a flexible polyimide diaphragm and CMOS buffers, is attached to the titanium base whenever electrical contact is required. The polyimide flexible diaphragm contains high-density gold electroplated pads (32 pads, each having an area of 100×100 μm^2 and separated by 150 μm) which match similar pads on the electrode back-end. When vacuum is applied between the two, the polyimide diaphragm deflects and the corresponding gold pads touch, therefore, establishing electrical connection. *In vitro* electrical tests in saline solution have been performed on a 32-site connector system demonstrating <5 Ω contact resistance, which remained stable after 70 connections, and -55 dB crosstalk at 1 kHz between adjacent channels. *In vivo* experiments have also confirmed the establishment of multiple contacts and have produced simultaneous biopotential recordings from the guinea pig occipital cortex.**

Index Terms— **Biomedical microsystems, high-density connectors, implantable devices.**

I. INTRODUCTION

A NUMBER of micromachined, multichannel neural probes and electrodes have been developed recently [1]–[5]. These probes are now capable of supporting several tens of recording or stimulating sites for interfacing with the nervous system. One of the main challenges in the application of these electrodes is the transfer of low-level, high source-impedance signals from the small sites to the outside world. Most implantable systems nowadays use hard-wired interconnections for signal transfer, which dictates that

T. Akin is with the Department of Electrical and Electronics Engineering, Middle East Technical University, TR-06531 Ankara, Turkey.

*B. Ziaie is with the Department of Electrical Engineering and Computer Science, Center for Integrated Sensors and Circuits, University of Michigan, Ann Arbor, Michigan 48109-2122 USA (e-mail: babak@engin.umich.edu).

S. A. Nikles is with the Department of Electrical Engineering and Computer Science Center for Integrated Sensors and Circuits and the Department of Biomedical Engineering, University of Michigan, Ann Arbor, Michigan 48109-2125 USA.

K. Najafi is with the the Department of Electrical Engineering and Computer Science, Center for Integrated Sensors and Circuits, University of Michigan, Ann Arbor, Michigan 48109-2122 USA.

a connector be attached to the animal [6]–[10]. Whenever interfacing with the probes is required, an external connector is attached to the subject and contact is made to individual sensors. Ideally, these connectors should satisfy a number of requirements. They should: 1) have a small footprint and a low profile, while still having a very high density; 2) be modular, with interchangeable parts so that when failure occurs in one component, only that component has to be replaced; 3) be removable, thus allowing connections to be made to the implant when desired; 4) be fabricated from biocompatible materials; 5) provide a means to buffer, and perhaps multiplex, the high-impedance signals of the sensors before sending them to the outside world; and, finally, 6) be low cost and easy to assemble.

Most of these requirements can be achieved by integrating on-chip circuitry on the probes (active probes) [11], [12]. However, these are harder to fabricate and do not lend themselves easily to frequent redesigns, as often needed by the biomedical community. Multichannel micromachined passive probes (i.e., probes without on-chip electronics) are now in widespread use worldwide [13]. Connection to the sites on most of these probes is achieved by wire bonding pads on the back-end of the probes to pins in an external connector, which is subsequently potted in epoxy [6]. However, bonding and insulating the back-end of the probe and connector complicates implant preparation, especially when a large number of output lines are required. In fact, most connectors with the exception of the PI Medical (Portland, OR) high-density connector system [10] which can transfer 64 leads out of the skin, have fewer than 12 pins. The PI Medical connector system lacks buffering capability and has a grid contact array area of 12.7×12.7 mm^2 (1.6-mm separation between the contacts) which is large for attachment to the skull of experimental mammals smaller than guinea pig [10]. The Microtech 12-pin connector (FR-12S-4, outer diameter of $\sim$9.5 mm) is used in some chronic applications. However, this connector is not considered a high-density connector and can not be easily scaled down to accommodate more contacts [13].

In order to overcome the aforementioned shortcomings, we have developed a high-density, modular, low-profile, small, removable connector system using micromachining technologies [14]. The connector simplifies implant preparation by eliminating the need for wire bonding and insulating materials, by incorporating buffer chips into the connector body, and by allowing several tens of output lines to be transferred to the outside world in a small, low-profile design. In Section II, the connector structure is described, followed by its design and
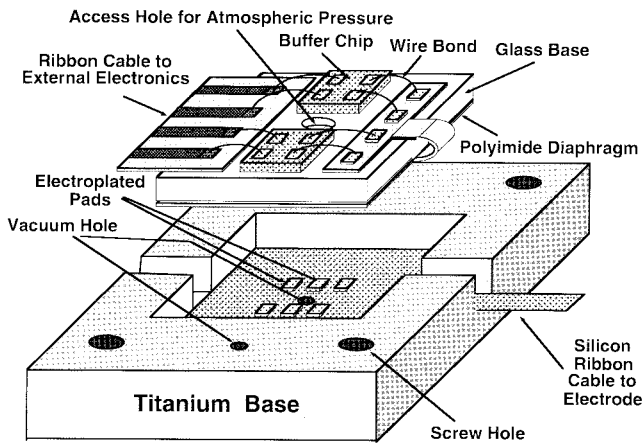
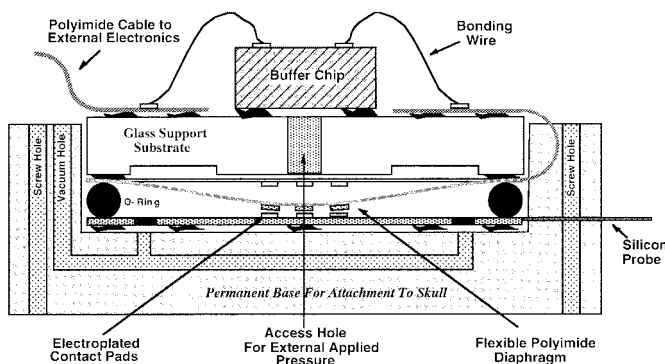Fig. 1.   Overall view of the high-density percutaneous connector system.

Fig. 2.   Cross-sectional view of the high-density percutaneous connector system.

fabrication in Section III. The assembly technique is discussed in Section IV, followed by *in vitro* and *in vivo* test and measurement results in Section V. Finally, Section VI draws some conclusions from the results of this work.

II. CONNECTOR STRUCTURE

Figs. 1 and 2 show the overall structure and cross-sectional view of the high-density percutaneous connector system, respectively. The connector system consists of three modular components: 1) a titanium base that is attached to the implant subject (the fixation site can be the skull or other anatomic locations depending on the application), 2) a silicon or polyimide micromachined probe for implantation in the biological tissue, and 3) an external micromachined connector that interfaces with the titanium base and the probe back-end and transfers the signals from/to the outside world. The sites on the probe are connected to the pads on its back-end using an integrated ribbon cable [15]. In one of the designs, this back-end measures 6×6 mm^2 and contains 32 electroplated 25-μm-thick 100×100 μm^2-sized gold pads. The electrode back-end is simply placed inside and attached onto the titanium base having a $6 \times 6 \times 0.74$-mm^3 recess. When interfacing with the implant is needed, the external connector is placed inside the recess in the base and held there by vacuum, as shown in Fig. 2.

The external connector consists of: 1) a 750-μm-thick glass substrate which has a circular recess (4 mm in diameter and 15 μm in depth), 2) a micromachined polyimide diaphragm, 3) two hybrid integrated circuit chips each containing 16 unity-gain CMOS buffers, and 4) a long polyimide cable for electrical connection to the external electronics (this cable is 30-cm long and was fabricated by Dynaflex Technology, San Jose CA). The polyimide diaphragm contains 25-μm-thick gold electroplated pads matching those on the electrode back-end, and is attached to the glass substrate (the 15-μm recess in the glass piece defines the diaphragm diameter). Electrical connection is achieved by drawing vacuum in the space between the electrode back-end and the polyimide diaphragm through a vacuum channel in the titanium base, as shown in Fig. 2. Note that the electrode back-end contains holes to provide access to the vacuum channel. A polyimide O-ring is also placed between the electrode back-end and the external connector to seal the perimeter when vacuum is applied. The applied atmospheric pressure on the polyimide diaphragm will force it to uniformly deflect until it bottoms out on the probe back-end thus providing electrical contact between the gold pads (an external mechanical force may also improve the connection; see Section V). The electroplated pads on the polyimide diaphragm are connected to unity-gain CMOS buffer chips. These buffers are placed on the back side of the glass substrate and connected to the diaphragm through a short multilead polyimide cable. This polyimide cable is an integral part of the polyimide diaphragm which supports the gold pads. The outputs of the buffers are connected to remotely located external electronics using a separate long polyimide cable.

This system offers several advantages. First, it is high density, allowing multiple signals to be transferred to the outside. Second, it is modular, with each piece being easily replaceable. Third, since there is no need for wire bonding or insulation over the electrode back-end, the connector can be low-profile. Fourth, the signal processing electronics are built right into the connector, thus, minimizing noise and effects of parasitics, which can have a significant impact on signal quality for neural recording applications. And finally, it requires minimal animal disturbance during multiple biological experiments. In Section III, we will discuss the design and fabrication of various components of the connector system.

III. DESIGN AND FABRICATION

Depending on the specific application, the recording probes can be fabricated from either polyimide or silicon. In situations where excessive bending and twisting is necessary during surgery or in contact with the biological tissue (e.g., cardiac recording), polyimide electrodes and cables offer certain advantages with regards to flexibility and durability. The shape and size of the probe depends on the needs of the investigator and can vary from needle-shaped probes for recording from cerebral cortex [1] to sieve-type probes used in nerve regeneration studies [6], [16]. The fabrication process for polyimide probes is similar to the polyimide external diaphragm and will be discussed in this section. The fabrication of the silicon recording probes has been reported elsewhere [1], and it is
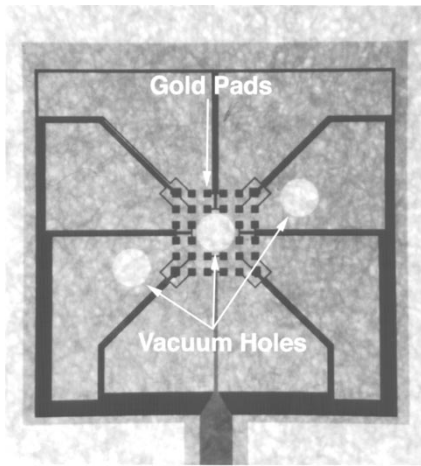
Fig. 3. A photograph of the back-end of a polyimide probe (6×6 mm^2 in area), which contains 32 electroplated gold pads (100×100 μm^2 separated by 150 μm) and three vacuum holes.

sufficient for our present discussion to only mention a few points. The probes are fabricated using the dissolved wafer process. The probe back-end and the shank are fabricated by a deep boron diffusion step ($\sim$15 μm) and the ribbon cable is fabricated by a shallow boron diffusion step ($\sim$3 μm). One extra mask is needed in order to electroplate gold ($\sim$25 μm) onto the back-end pads. The back-end should be slightly smaller (by about 25 μm on each side) than the size of the recess in the titanium base. This is due to lateral diffusion during the deep boron diffusion step. We have fabricated silicon and polyimide probes with modified back-end in order to accommodate high-density pad grid array and vacuum holes. Fig. 3 shows a photograph of the back-end of a polyimide probe, which contains 32 electroplated gold pads and three vacuum holes.

The shape and the size of the titanium base is dictated by the animal model and implantation site (one has also to take into account skin thickness, downgrowth, and recession) [17]. For example, a base mounted on the skull of a rat should be no larger than 5×5 mm^2, whereas the guinea pig skull can house larger bases. In one of the prototypes designed for recording neural activity from the guinea pig cortex, the implanted titanium base is cylindrical in shape and has a diameter of 12.5 mm and a height of 2.5 mm. The height and the shape of the base might have to be modified (e.g., adding flanges and grooves) to promote tissue growth and stabilization. The base is precision machined and has a recess of 0.74 mm to house the electrode back-end and the glass substrate of the external micromachined connector. The titanium base also contains a channel which is used to pull vacuum between the polyimide diaphragm and the electrode.

The glass substrate part of the external connector has the same dimensions as the recess in the titanium base and the electrode back-end and is fabricated from #7740 Corning glass wafers. First, the glass wafer is patterned, and a 15-μm-deep recess is etched into it in the area above the connection pads. Then a hole is drilled in the middle of the recess, and finally, the glass is diced. The hole is required to expose the back side of the polyimide diaphragm to atmospheric pressure so that
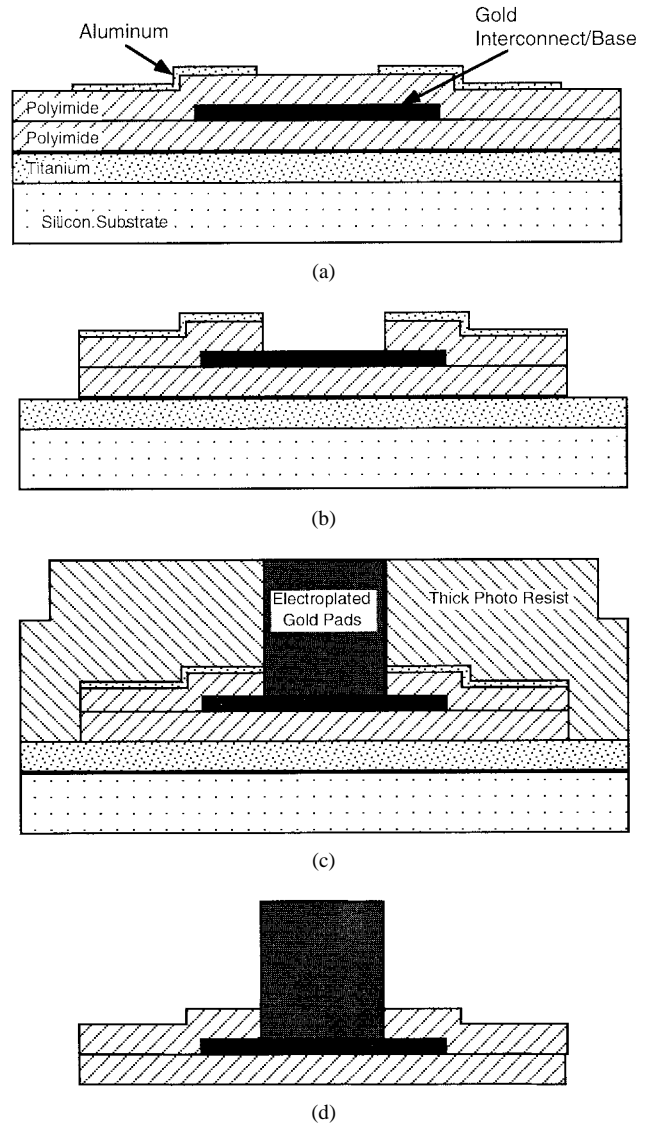

Fig. 4. Fabrication process of the polyimide diaphragm: (a) evaporate Ti, spin bottom polyimide, evaporate and pattern Cr/Au/Cr, spin top polyimide, evaporate masking Al for RIE; (b) RIE etch polyimide; (c) spin and pattern 18 mm-thick photoresist, electroplate gold pads; and (d) etch Ti in 20% HF and 80% DI water to release the structure.

when vacuum is applied the diaphragm can deflect; the hole can also be used to apply additional pressure on top to obtain a better contact.

Fig. 4 shows the fabrication process of the polyimide diaphragm. It starts by evaporating a 1-μm-thick sacrificial titanium (Ti) layer on a silicon wafer. Then, the 4-μm-thick bottom polyimide layer (PI 2611, DuPont, Wilmington DE) is deposited and cured (5 min at 120 °C, 5 min at 180 °C, and 1 h at 400 °C, all on a hot-plate in a cleanroom environment). Next, a Cr/Au/Cr (400 Å/4000 Å/200 Å) interconnect layer is evaporated. After patterning the Cr/Au/Cr interconnect layer, the 4-μm-thick top polyimide is deposited and cured. Then, a 3000-Å aluminum masking layer is deposited and patterned for masking the polyimide etch in RIE (O$_2$ flow $= 100$ sccm, power $= 300$ W, pressure $= 200$ mTorr). Next, a 25-μm-thick photoresist (PR4620) is deposited on the wafer and patterned. A gold layer is electroplated in the open pad areas

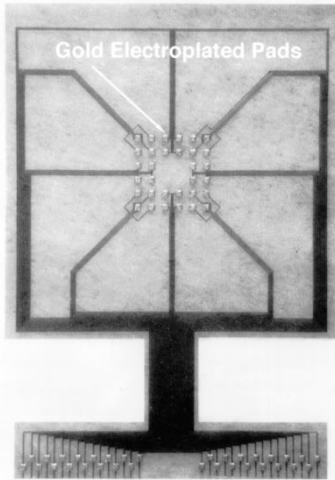Fig. 5. A photograph of a fabricated polyimide diaphragm, which contains 32 100×100 μm^2 gold pads.

Fig. 6. A photograph of the glass substrate which contains the buffer chips and the polyimide diaphragm placed inside the titanium base.

(55 °C plating bath and 2-mA/cm^2 current density). Finally, the devices are released from the wafer by etching the initial titanium sacrificial layer in a mixture of hydrofluoric acid (HF) and deionized (DI) water (20%HF/80%DI). Fig. 5 shows a photograph of a fabricated polyimide diaphragm, which contains 32 100×100-μm^2 gold pads. As was mentioned previously, the same process can be used to fabricate polyimide probes and ribbon cables.

The central deflection of the polyimide diaphragm should be large enough to ensure electrical contact when one atmosphere of pressure is applied. This depends on the thickness of the O-ring located between the electrode back-end and the polyimide diaphragm, as shown in Fig. 2. Since O-rings thinner than 100 μm are usually used in this application ($\sim$40 μm in one of our designs), a center deflection of $\sim$100 μm will suffice for contact. Equation (1) relates the central deflection of a circular diaphragm to applied pressure, as a function of material properties [18]

$$\frac{Pa^4}{Eh^4} = \frac{16y}{3(1-\nu^2)h} + \frac{(7-\nu)y^3}{3(1-\nu^2)h^3} + \frac{4a^2sy}{(1-\nu)Eh^3}. \quad (1)$$

In this equation P is the applied pressure, E is the Young's modulus, ν is the Poisson's ratio, h is the diaphragm thickness, y is the center deflection, a is the diaphragm radius, and s is the internal stress of the diaphragm material. According to the published data, Young's modulus and stress for the PI-2611 polyimide are 8.3 GPa and 9 MPa, respectively [19]. Using (1), a diameter of at least 2.5 mm is required for an 8-μm-thick polyimide diaphragm to deflect 100 μm when 1 atm. of pressure is applied. The external connector used in our application provides a diaphragm diameter of about 4 mm, which should provide sufficient deflection to achieve contact between the diaphragm and the electrode.

IV. ASSEMBLY

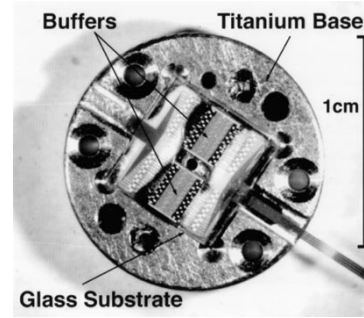The connector assembly starts with the preparation of the recording probe and the titanium base. The base is thoroughly cleaned with acetone and isopropyl alcohol (IPA) in order to remove any particulates. The presence of any large particulates underneath the silicon electrode back-end can cause its breakage when the external connector is placed on top of it. After cleaning the base, the probe back-end is glued to the recess in the base using a fast setting epoxy. Notice that in the event of a silicon probe breakage either during assembly or surgery, one can easily replace it without having to discard or remove the titanium base. This is a very important feature of this connector system, because it allows the user to fix the titanium base to the subject and use it with different types of probes.

After the electrode/titanium-base is prepared and attached to the subject, the external connector is assembled. First a small amount of epoxy is applied around the perimeter of the glass piece under the microscope. Then, the glass piece is placed in the titanium base recess on top of the electrode back-end using a vacuum pick. The polyimide diaphragm is then placed on the glass piece, and the bonding pads on the polyimide and electrode are aligned under the microscope. Following the hardening of the epoxy, the other end of the polyimide piece which contains the bonding pads for the connection to the buffer inputs is folded over and glued to the top of the glass piece. The two CMOS buffer chips, each with 16 buffer-connected operational amplifiers, are next attached to the glass piece on either side of the drilled hole. Finally, the assembly of the external connector is completed by attaching a long polyimide cable ($\sim$10 to 30-cm long) to the glass for connection to the external electronics and coating the buffers with a protective layer of epoxy. This cable should be long enough to produce a minimum amount of bending moment and force on the glass. Another important advantage of this system is that there is no need for alignment of the glass and probe back-end when a recording is desired. This is because they are both mechanically aligned to the sidewalls of the titanium base. The accuracy of this alignment will determine the ultimate density of the interconnects for this connector. Using this simple technique it is easily possible to obtain alignment accuracy of at least 50 μm, allowing the implementation of a connector system with higher number pads located in the same area as the 32-pad system (for example 64), with smaller contact pads areas and smaller separation.

Fig. 6 shows a photograph of the glass substrate which contains the buffer chips and the polyimide diaphragm placed
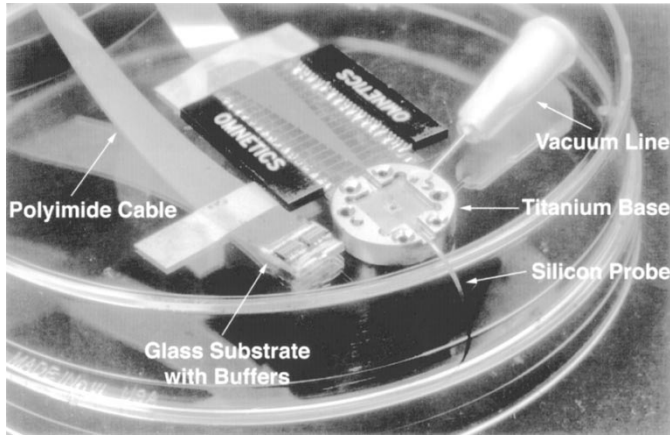
Fig. 7. A photograph of the complete connector system (Omnetics connector is attached to the other end of the long polyimide cable for interfacing with the outside electronics).

inside the titanium base. Note that there is a hole in the glass which provides access to the back side of the polyimide diaphragm. An extra protective cap (not shown here) can be used to cover the electrode back-end when recording in not required. This will help to keep the fluids and particulates out of the titanium base and electrode back-end. Fig. 7 shows a photograph of the complete connector system. A silicon cable and probe are clearly visible, and the top glass substrate which is the external portion of this connector is placed alongside the titanium base. The tube which provides vacuum access is also shown.

V. TEST RESULTS

In vitro tests to characterize the connector system for important electrical parameters and *in vivo* neural recordings to prove the operation of the system in a real biological environment have been performed.

A. In Vitro Tests

Extensive *in vitro* electrical tests to measure contact resistance, crosstalk, and reliability have been performed on a completed connector system. These three are the most important performance parameters for connectors used in implantable systems.

1) Contact Resistance Measurements: The contact resistance was measured using a specially constructed setup. A polyimide piece containing 32 gold electroplated pads (100×100 μm each) was glued in a titanium base, where the back-end of a probe would normally be placed. The polyimide piece was used instead of a probe so that the channels could easily be connected to external circuitry. An external connector was assembled as described in Section IV, including a glass substrate, a diaphragm, and a polyimide cable (no buffers were used in this case). The resistance of each channel was measured under a probe station on both the polyimide piece in the titanium base, and the external connector. Next, the external connector was placed in the base, vacuum was drawn between the two pieces, and the total series resistance of each channel was measured. The contact resistance was calculated

by subtracting the resistances of the polyimide piece in the base and the external connector from the total resistance for each corresponding channel. The external connector was then removed and reattached 70 times, measuring five channels each time for a total of 350 measurements. None of the five channels failed to connect during any of the 70 trials. After every tenth trial, the gold pads in the titanium base were rinsed with saline solution, dried, rinsed three times with DI water, and dried again. This was done to simulate the effect of fluids getting into the base between recordings. The average contact resistance was found to be 2.2 ± 1.7 Ω for each channel. Furthermore, no significant change in contact resistance could be noticed during the 70 trials. The contact resistance under current stimulation conditions was also measured using a charge balanced current waveform with a cathodic peak of 4.3 mA. The current source was connected to five channels separately for 10 s each and the contact resistance was measured for each channel 30 times. The contact resistance was measured to be 1.9 ± 1.8 Ω and no significant change in the contact resistance was noticed after 30 trials.

2) Crosstalk Measurements: It is extremely important to ensure that the crosstalk between individual channels of the connector is low ($<1\%$ is adequate for most applications) to ensure acceptable quality recording of neural signals which are of low amplitude and high impedance in nature. The crosstalk between adjacent channels was analyzed using the electrical equivalent circuit model of the connector system, shown in Fig. 8(a). This model shows the elements that are most pertinent to analyzing the crosstalk, including: V_s and R_s, corresponding to the bioelectric voltage source and solution resistance, respectively; R_e and C_e, representing the electrode impedance; R_i, representing the electrode lead series resistance; C_s, representing shunt capacitance from the electrode leads to the substrate and solution; C_p and C_d, corresponding to the crosstalk capacitances between adjacent lines in the electrode and polyimide diaphragm; and, finally, C_c, representing the crosstalk capacitance in the long polyimide external cable. The effect of C_c on the crosstalk is negligible due to the impedance transformation effect of the buffers (low output impedance). This means that most of the crosstalk is due to the capacitive coupling occurring in the electrode and polyimide diaphragm. Therefore, the only important parameters are the electrode impedance, shunt capacitances to ground, and the crosstalk capacitance between adjacent lines. The metallic interconnect and solution series resistances and the input resistance of the buffers for the most part can be neglected. The effect of the input capacitance of the buffers can be included by adding its value to the shunt capacitances (C_s). Fig. 8(b) shows a simplified model for crosstalk analysis incorporating the above simplifications (the electrode impedance is represented by Z_e which includes both C_e and R_e, and C_t is the sum of C_p and C_d). The crosstalk voltage ratio is given by

$$\frac{V_2}{V_1} = \frac{j\omega C_t}{j\omega(C_t + C_{s2}) + 1/Z_{e2}}. \quad (2)$$
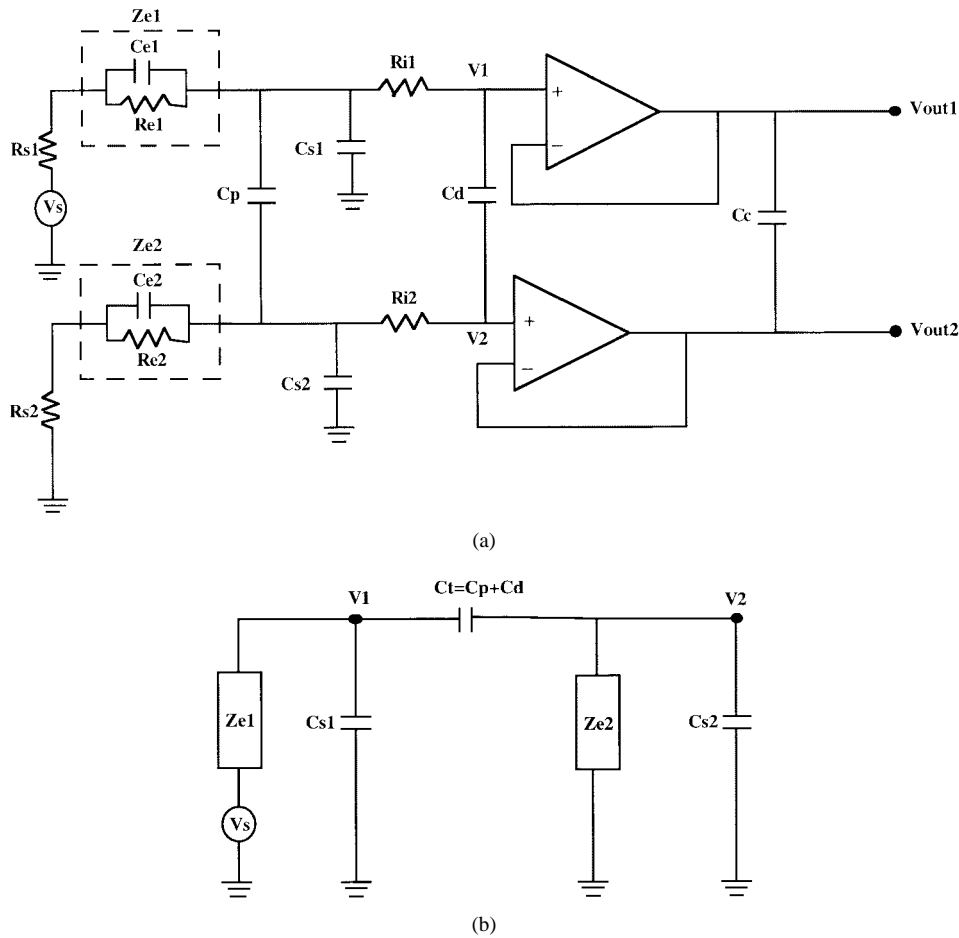
Fig. 8. (a) Electrical equivalent circuit model of the connector system for crosstalk analysis (see the text for the description of various components) and (b) a simplified model.

In most practical cases, $Z_{e2} \ll 1/j\omega(C_t + C_{s2})$. Therefore, (2) can be reduced to the following:

$$\frac{V_2}{V_1} = j\omega Z_{e2} C_t. \tag{3}$$

Equation (3) shows that crosstalk is directly proportional to the frequency, the electrode impedance, and the capacitance between the conductors. Assuming an electrode impedance of 500 kΩ, the crosstalk capacitance must be less than 3 pF in order to keep the crosstalk level below 1% at 1 kHz. This can easily be achieved by proper spacing between the conductors in the electrode ribbon cable and polyimide diaphragm. It has been shown that as long as the distance between two adjacent lines is greater than the width of the lead wire, the crosstalk capacitance is less than 0.5 pF/cm and, therefore, is acceptable for path lengths up to 6 cm [20].

Electrical crosstalk between two adjacent channels was measured to be −55 dB (at 1 kHz) with the electrode outside the solution and terminated with a 470-kΩ resistor. This technique was chosen due to the difficulty of selectively applying a local potential to a site while the electrode is in a saline bath. The electrode had a length of approximately 20 mm. At the electrode tip the line width and spacing were 3 and 2.5 μm, respectively (becoming 6 μm each on the ribbon cable), compared to 20-μm width and 6-μm spacing

on the polyimide diaphragm. Crosstalk was again measured after applying saline to the titanium base recess, removing the saline and a complete nitrogen dry (this was performed in order to mimic the actual operating environment of the connector which could possibly contain bodily fluids). The second measurement yielded a crosstalk of −50 dB (at 1 kHz). Both of these values indicate that excellent isolation can be achieved between adjacent channels.

3) Reliability Tests: Two quantities of particular importance in the high-density connector are single pad reliability (SPR) and multiple pad reliability (MPR). SPR is defined as the percentage of the time that a *single* channel (i.e., contact pad) makes a low–resistance contact over *all* performed trials, and MPR is defined as the percentage of *all* the channels that connect during a *single* trial. Tests were performed to determine both the single and multiple pad reliabilities using various attachment conditions. These included application of vacuum, incorporation of an O-ring, or application of mechanical pressure (applied by pressing down on the external connector). Each test consisted of several trials involving the connection and disconnection of the external connector from the titanium base, while checking for continuity of each channel. It should be mentioned that prior to each test, channels in both the titanium base and the external connector were individually tested for continuity and broken channels
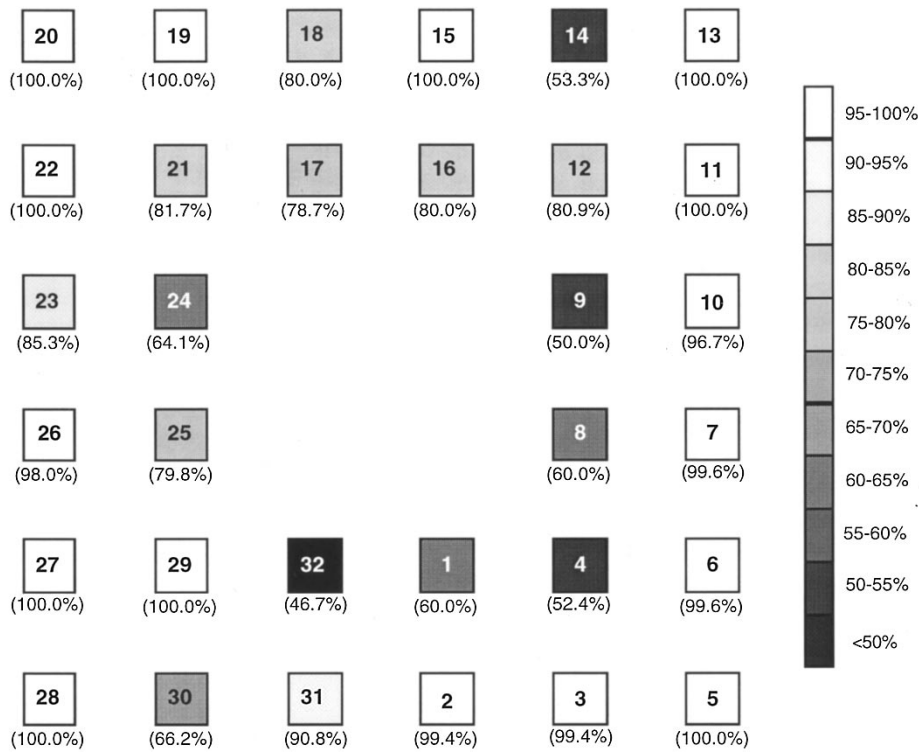
Fig. 9. The plot of SPR against the pad locations on the diaphragm.

TABLE I
OVERALL SINGLE PAD AND MULTIPLE PAD
RELIABILITIES FOR VARIOUS ATTACHMENT CONDITIONS

Vacuum	O-ring	Mechanical Pressure	Overall SPR	Overall MPR
--	--	--	21.2%	21.5%
YES	--	--	59.5%	76.1%
--	--	YES	63.6%	62.7%
YES	--	YES	82.0%	78.9%
YES	YES	--	23.4%	29.3%
YES	YES	YES	84.5%	82.1%

(which had either no gold pad or bad wire bonds) were excluded from the study. It was noticed that both the MPR and SPR are dependent upon the attachment conditions used, i.e., the manner in which the external connector is attached to the titanium base, as summarized in Table I. The conditions that produced the best results were those that used vacuum, O-ring, and mechanical pressure, simultaneously. The worst results occurred when nothing was used at all (still, on average 21.5% of the pads made a connection each trial).

Six connector assemblies were tested under the best attachment conditions. Some assemblies had as many as 41 trials performed on them, however, not all assemblies tested had as many trials (the average number of trials performed under these conditions was 13). The MPR for each trial was calculated as the number of channels that made a connection, divided by the number of all possible channels. These were then averaged over all trials performed on the assemblies to give the average MPR. This yielded an overall MPR of 82.1%, which may be interpreted as the average percentage of channels one would expect to work for a newly assembled connector. After all trials had been performed, the SPR was calculated for each channel. The SPR's for all 32 channels

were taken over all assemblies tested. This indicates which channels are most likely to make a connection during each trial. Fig. 9 shows the pad locations on the diaphragm and SPR results. Of the 32 channels, 17 connected more than 90% of the time, while the worst channel connected only 47%. The overall SPR was calculated to be 84.5%. This value may be interpreted as the average probability with which any one pad will connect in a newly assembled connector.

Although the above reliabilities are quite high in many cases, there are still some channels that do not connect adequately. In order to investigate the possible reasons for the low connection rates for these channels, the SPR was plotted against the pad locations on the diaphragm, as shown in Fig. 9. In this figure, each square represents a contact pad, numbered from 1 to 32, and the SPR value for a given pad is shown below it. As can be seen, those pads in the outer perimeter tend to connect more often than those in the center (in many cases those pads connect 100% of the time). One possibility for this behavior is that due to the uneven application of vacuum the diaphragm in the external connector buckles in the center when it comes into contact with the probe back-end. Note that there exist three vacuum holes in the probe back end (Fig. 3), two of them are located diagonally on the outside of the square that bounds the contact pads. It is possible that when vacuum is applied, the outside perimeter is pulled down more forcefully thus buckling the membrane in the center and reducing the probability of contact. This could be corrected by relocating the vacuum holes in the base, thus altering the distribution of force on the diaphragm (e.g., removing two diagonal holes and using only a single central hole). Table I also shows that although the best results were

obtained when an O-ring was used and both vacuum and mechanical pressure were applied, the case when no O-ring was used and only vacuum or both vacuum and pressure were applied also provided very good results. Although, we have been able to construct several connectors in which all of the channels connected every time (100% MPR and SPR), the reproducibility has not been consistent. We believe that this is primarily due to the position of the vacuum holes in the substrate, as mentioned before, and partially to the care taken when assembling the titanium base and attaching the probe back end. It is also interesting to note that the application of mechanical pressure alone also provides good contact and is a technique which should be pursued for future systems.

B. In Vivo Tests

In order to evaluate the connector functionality *in vivo*, bio-electrical recordings from the occipital cortex of a guinea pig were performed. The guinea pig was initially anesthetized with ketamine hydrochloride (Vetalar, 100 mg/kg) and xylazine (Rompun, 5 mg/kg) delivered intramuscularly and supplemented regularly to maintain appropriate levels of anesthesia. The animal was placed on a DC-powered heating pad, which maintained core body temperature at 37.5 °C using feedback from a temperature probe. After removing the scalp, the exposed skull was stabilized by threading stainless steel screws into the dorsal cranium. These were embedded in methyl methacrylate dental acrylic (Lang Dental Mfg., Wheeling, IL) and attached to a fixed rigid bar. An opening in the cranium was made with a drill and then enlarged with bone rongeurs. The dura was removed to expose the occipital cortex. Next, the titanium base was attached to the skull using a stainless-steel screw. Dental wax (Moder Materials Mfg. Co., St. Louis, MO) was used to further secure the base. A 32-channel polyimide recording electrode had already been attached to the base at this point. The recording electrode was then carefully inserted through the cortex toward the inferior colliculus. The animal was grounded by inserting a needle electrode into its dorsum. The polyimide O-ring and external connector were then placed in the recess of the titanium base and vacuum was turned on, thus establishing connection. Fig. 10 shows the connector attached to the guinea pig skull with the probe extending into the cortex.

After passing each channel through a unity-gain CMOS buffer on the connector system, the recorded signals were sent through a 16-channel external data acquisition system. Each channel in this system consists of: a preamplifier (1000×, a second amplifier (adjustable gain of 1×, 3×, or 10×), and a bandpass filter (100 to 10 000 Hz to remove low- and high-frequency noise). Fig. 11 shows 16-channel biopotentials recorded from the probe using the high-density connector system. Note that channel 8 was used as a reference for differential recording and channel 12 was inoperative due to a damaged buffer. The waveform on channel 4 shows spontaneous neural activity, indicating that the recording site for that channel was near a firing neuron in the cortex. The remaining channels show what appears to be background neural noise. This indicates that the channels were functional,
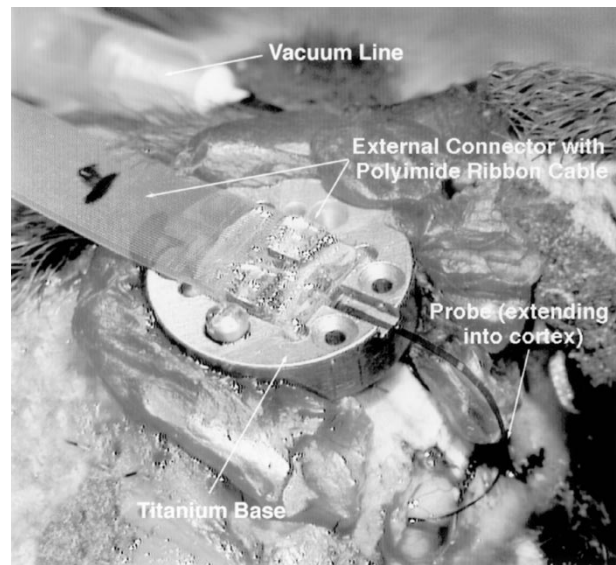

Fig. 10.   A photograph showing the connector system on top of a guinea pig skull and a polyimide probe penetrating the occipital cortex.

but their individual recording sites were not situated near any firing neurons. A small amount of crosstalk between channel 4 and its neighbors is evident after close inspection. However, this is more than the expected value from crosstalk calculations (−55 dB), which implies that the adjacent channels are picking up this activity directly from the active neuron near the recording site of channel 4. In order to test the measurement repeatability, the external connector was removed and placed back into the recess several times. In addition, the probe back-end became wet during surgery, requiring several cleaning and dry out steps. This multiple manipulation did not change the signal and noise levels, proving the short-term reliability of the system under harsh recording conditions.

VI. DISCUSSION AND CONCLUSION

A percutaneous high-density connector system has been developed. It consists of three modular components: 1) a titanium base that is attached to the implant subject, 2) a micromachined probe for implantation in the biological tissue, and 3) an external micromachined connector that interfaces with the probes and transfers their signals to the outside world. Electrical connection between the recording sites on the electrode and the external electronics is established upon the application of vacuum between a polyimide diaphragm on the external connector and the electrode back-end. The pressure gradient deflects the diaphragm causing high-density gold electroplated pads on the polyimide to touch those on the electrode. Electrical measurements have shown a low contact resistance ($<5\ \Omega$) between the pads and a crosstalk of −55 dB between adjacent channels for the electrodes used in this experiment. The contact resistance remained stable after 70 and 30 insertions under recording and stimulating conditions, respectively. The connector reliability was evaluated by performing multiple insertion tests and measuring two important reliability dependent parameters, i.e., SPR and MPR.
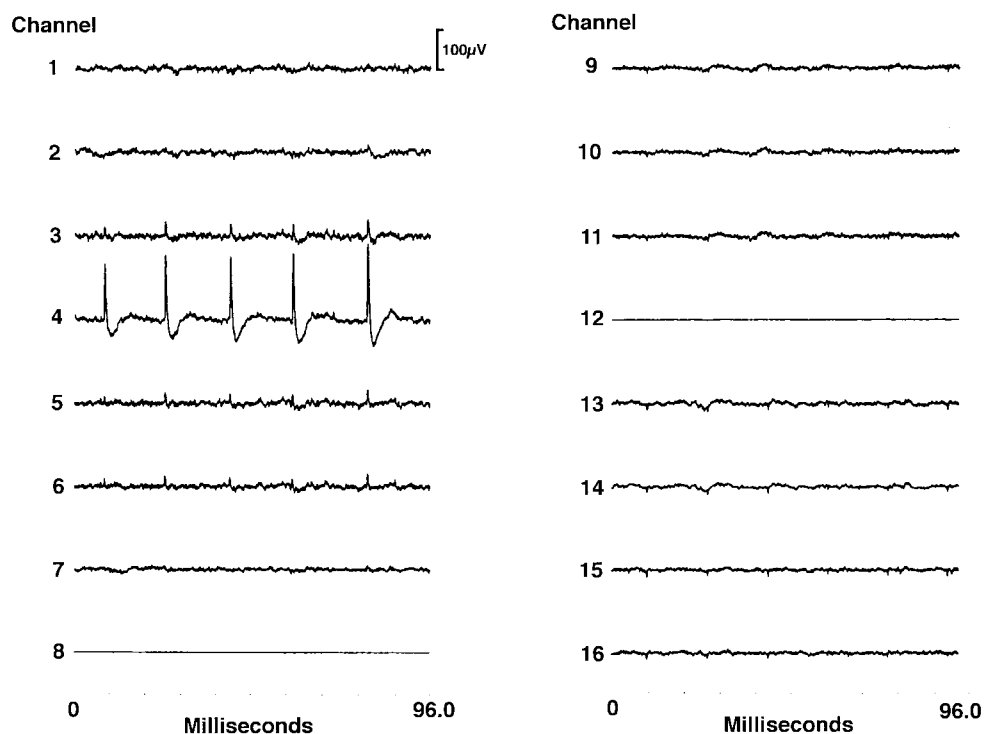
Fig. 11. Biopotential recordings from the guinea pig occipital cortex, showing simultaneous neural background activity on 14 channels upon application of vacuum to the connector system.

Six connector assemblies were tested under best attachment conditions (vacuum, O-ring, and mechanical pressure), SPR and MPR were measured to be 84.5% and 82.1%, respectively. We believe one can improve the reliability by: 1) redesigning the titanium base and probe back-end for a better and more uniform vacuum application and 2) further simplifying the assembly process by integrating more components into single units (e.g., the glass piece can be substituted by silicon thus allowing the buffers to be integrated with the top polyimide diaphragm into a single unit). *In vivo* experiments have also confirmed the establishment of multiple contacts and simultaneous biopotential recordings from the guinea pig occipital cortex. We are currently preparing for long-term chronic recordings which should answer questions regarding long-term stability and biocompatibility of the connector system.

This connector system offers several important advantages compared to the existing percutaneous systems. These include: 1) higher-density, 2) modularity, 3) lower-profile, and 4) reduced volume. The connector can easily be extended to include more channels. In addition, by attaching a swivel to the long external polyimide cable, one can record from a freely moving animal without the risk of twisting and tangling the connection. The application of vacuum and O-ring can be avoided by electroplating the contact pads high enough in order for them to touch upon the placement of the external piece. One can also use a spring backing mechanism or magnetic actuation to apply force and deflect the diaphragm, therefore, removing the need for vacuum application. We believe this connector system is a significant advance for implantable biomedical systems and clearly demonstrates the application of microelectromechanical (MEMS) technology to solve important biomedical problems. The results of this work can be used in other applications where small high-density connectors are needed. These may include: diagnostic tests on large element arrays like ultrasound imaging transducers, active matrix flat panel displays, and probe station testing of VLSI circuits with large number of output pads.

REFERENCES

[1] K. Najafi, K. D. Wise, and T. Mochizuki, "A high-yield IC-compatible multichannel recording array," *IEEE Trans. Electron Devices*, vol. ED-32, pp. 1206–1211, May 1985.
[2] G. T. A. Kovacs, C. W. Storment, M. H. Miller, C. R. Belczynski, C. C. Della Sentina, E. R. Lewis, and N. Maluf, "Silicon-substrate microelectrode arrays for parallel recording of neural activity in peripheral and cranial nerves," *IEEE Trans. Biomed. Eng.*, vol. 41, pp. 567–577, June 1994.
[3] C. T. Nordhausen, E. M. Maynard, and R. A. Norman, "Single unit capabilities of a 100 microelectrode array," *Brain Res.*, vol. 726, pp. 129–140, 1996.
[4] A. L. Owens, T. J. Denison, H. Versnel, M. Rebbert, M. Peckerar, and S. Shamma, "Multi-electrode array for measuring evoked potentials from surface of ferret primary auditory cortex," *J. Neurosci. Meth.*, vol. 58, pp. 209–220, 1995.

[5] N. A. Blum, B. G. Carkhuff, H. K. Charles, R. L. Edwards, and R. A. Meyer, "Multisite microprobes for neural recordings," *IEEE Trans. Biomed. Eng.*, vol. 38, pp. 68–74, Jan. 1991.

[6] R. M. Bradley, X. Cao, T. Akin, and K. Najafi, "Long term chronic recordings from peripheral sensory fibers using a sieve electrode array," *J. Neurosci. Meth.*, vol. 73, pp. 177–186, 1997.

[7] K. Akazawa, M. Makikawa, J. Kawamura, and H. Aoki, "Functional neuromuscular stimulation system using an implantable hydroxyapatite connector and a microprocessor-based portable stimulator," *IEEE Trans. Biomed. Eng.*, vol. BME-36, pp. 746–753, July 1989.

[8] T. J. Koh, and T. R. Leonard, "An implantable electrical interface for *in vivo* studies of the neuromuscular system," *J. Neurosci. Meth.*, vol. 70, pp. 27–32, 1996.

[9] *Biomedical Product Catalog*, Konigsberg Instrument Inc., Pasadena, CA, Mar. 1994, p. 6.

[10] "Development of a percutaneous connector system," in *Final Report*, PI Medical, Portland, OR, submitted to the National Institutes of Health.

[11] J. Ji, K. Najafi, and K. D. Wise, "A low-noise demultiplexing system for active multichannel microelectrode arrays," *IEEE Trans. Biomed. Eng.*, vol. 38, pp. 75–81, Jan. 1991.

[12] J. Ji and K. D. Wise, "An implantable CMOS circuit interface for multiplexed multielectrode recording array," *IEEE J. Solid-State Circuits*, vol. 27, pp. 433–443, Mar. 1992.

[13] D. J. Anderson, Director, Center for Neural Communication Technology, University of Michigan, 1301 Beal Av., Ann Arbor 48109, World Wide Web internet homepages: http://www.engin.umich.edu/facility/cnct/.

[14] T. Akin, B. Ziaie, and K. Najafi, "A modular micromachined high-density connector for implantable biomedical systems," in *Proc. IEEE Int. Workshop on Microelectromechanical Systems*, San Diego, Feb. 1996, pp. 497–502.

[15] J. F. Hetke, J. L. Lund, K. Najafi, K. D. Wise, and D. J. Anderson, "Silicon ribbon cables for chronically implantable microelectrode arrays," *IEEE Trans. Biomed. Eng.*, vol. 41, pp. 314–321, Apr. 1994.

[16] T. Akin, K. Najafi, R. Smoke, and R. Bradley, "A micromachined silicon sieve electrode for nerve regeneration applications," *IEEE Trans. Biomed. Eng.*, vol. 41, pp. 305–313, Apr. 1994.

[17] A. F. von Recum, "Applications and failure modes of percutaneous devices: A review," *J. Biomed. Mat. Res.*, vol. 18, pp. 323–336, 1984.

[18] M. Di Giovani, *Flat and Corrugated Diaphragm Design Handbook*. New York: Marcel Dekker, 1982.

[19] H. K. Charles, "Electronic packaging applications for adhesives and sealants," in *Engineering Materials Handbook*, vol. 3, H. F. Brinson, Ed. Metals Park, OH: ASM Int., 1990.

[20] O. J. Prohaska, F. Olcaytug, P. Pfundner, and H. Dragaun, "Thin-film multiple electrode probes: Possibilities and limitations," *IEEE Trans. Biomed. Eng.*, vol. BME-33, pp. 223–229, Feb. 1986.

Tayfun Akin was born in Van, Turkey, in 1966. He received the B.S. degree in electrical engineering with high honors from Middle East Technical University, Ankara, Turkey, in 1987 and went to the United States in 1987 for graduate studies with a graduate fellowship provided by NATO Science Scholarship Program through the Scientific and Technical Research Counsel of Turkey (TUBITAK). He received the M.S. degree in 1989 and the Ph.D. degree in 1994 in electrical engineering, both from the University of Michigan, Ann Arbor.

Since 1995, he has been employed as an Assistant Professor in the Department of Electrical and Electronics Engineering at Middle East Technical University. His research interests include analog and digital integrated circuit design, silicon-based integrated sensors and transducers, infrared detectors, and implantable microtelemetry systems and transducers for biomedical applications.

Dr. Akin was the winner of the First Prize in Experienced Analog/Digital Mixed-Signal Design Category at the 1994 Student VLSI Circuit Design Contest organized and sponsored by Mentor Graphics, Texas Instruments, Hewlett-Packard, Sun Microsystems, and Electronic Design Magazine. In 1996, he received the Research and Encouragement Award, given by the Prof. Dr. Mustafa N. Parlar Education and Research Foundation for "his original work in microelectronics and microsensors."

Babak Ziaie (A'95) received the B.S.E.E. degree from Tehran University, Tehran, Iran, in 1986 and the M.S. and Ph.D. degrees from the University of Michigan, Ann Arbor, in 1992 and 1994 respectively. His Ph.D. thesis concentrated on the design and development of a single channel microstimulator for functional neuromuscular stimulation. In 1994–95 he was a postdoctoral research fellow at the Cardiac Rhythm Management Laboratory at the University of Alabama, Tuscaloosa, where he was involved in developing high-density recording electrode arrays for mapping cardiac arrhythmia.

Since 1995 he has been employed as a Research Scientist at the Center for Integrated Sensors and Circuits, Department of Electrical Engineering and Computer Science, University of Michigan, where he has been involved in research and development of integrated sensors and actuators, microstructures, microtelemetry systems for biomedical applications, and packaging and encapsulation of implantable sensors. His major areas of interest include solid-state integrated sensors, micromachining technologies, VLSI and custom integrated circuits, instrumentation, and biotelemetry.

Dr. Ziaie is a member Tau Beta Pi and the American Association for the Advancement of Science.

Stefan A. Nikles received the B.S. degree in applied science-materials and the B.S. degree in physics in 1996 from the University of North Carolina, Chapel Hill. He is currently working towards the Ph.D. degree in biomedical engineering at the University of Michigan, Ann Arbor.

His research activities include development of micromachined sensors and actuators, and microsystems for biomedical applications.

Khalil Najafi (S'84–M'86–SM'97) was born in 1958. He received the B.S., M.S., and Ph.D. degree in 1980, 1981, and 1986 respectively, all in electrical engineering from the Department of Electrical Engineering and Computer Science, University of Michigan, Ann Arbor.

From 1986 to 1988, he was employed as a Research Fellow; from 1988 to 1990, as an Assistant Research Scientist; from 1990 to 1993, as an Assistant Professor; from 1993 to 1998, as an Associate Professor; and since 1998, as a Professor in the Center for Integrated Sensors and Circuits, Department of Electrical Engineering and Computer Science, University of Michigan. His research interests include: microfabrication and micromachining technologies for solid-state integrated sensors and microactuators; analog and digital integrated circuits; implantable microtelemetry systems and transducers for biomedical applications and wireless communication; technologies and structures for microelectromechanical systems (MEMS) and microstructures; hermetic packaging techniques for microtransducers; and low-power wireless sensing/actuating systems. He is an Associate Editor for the *Journal of Micromechanics and Microengineering*, Institute of Physics Publishing.

Dr. Najafi was awarded a National Science Foundation Young Investigator Award from 1992–1997. He was the recipient of the Beatrice Winner Award for Editorial Excellence at the 1986 International Solid-State Circuits Conference and of the Paul Rappaport Award for co-authoring the Best Paper published in the IEEE TRANSACTIONS ON ELECTRON DEVICES. In 1994, he received the University of Michigan's "Henry Russel Award" for outstanding achievement and scholarship. He was selected by students in the electrical engineering and computer science department as the "Professor of the Year" in 1993. He has been active in the field of solid-state sensors and actuators for 15 years and has been involved in several conferences and workshops dealing with solid-state sensors and actuators, including the International Electron Devices Meeting, the Hilton-Head Solid-State Sensors and Actuators Workshop, and the IEEE/ASME Microelectromechanical Systems (MEMS) Workshop. He is the Editor of Solid-State Sensors for IEEE TRANSACTIONS ON ELECTRON DEVICES.